

Four- and three-body channel coupling effects on ${}^6\text{Li}$ elastic scattering with CDCC

Shin Watanabe^{1,a}, Takuma Matsumoto¹, Kosho Minomo², Kazuyuki Ogata², and Masanobu Yahiro¹

¹*Department of Physics, Kyushu University, Fukuoka 812-8581, Japan*

²*Research Center for Nuclear Physics (RCNP), Osaka University, Ibaraki 567-0047, Japan*

Abstract. We investigate breakup dynamics in ${}^6\text{Li}$ elastic scattering on heavy targets ($T = {}^{209}\text{Bi}$ or ${}^{208}\text{Pb}$) near the Coulomb barrier energy. Since the subsystem of ${}^6\text{Li}$ has a bound state as deuteron ($n + p = d$), a four-body channel (${}^6\text{Li} + T \rightarrow n + p + \alpha + T$) and a three-body channel (${}^6\text{Li} + T \rightarrow d + \alpha + T$) get entangled during scattering as a breakup channel. Both channels are precisely treated with the four-body version of the continuum-discretized coupled-channels method (four-body CDCC). Four-body CDCC well reproduces measured elastic cross sections with no adjustable parameter. We then estimate the channel coupling effects by dividing the breakup channel into four- and three-body channels. It is found that ${}^6\text{Li}$ breakup is mainly induced by a three-body channel.

1 Introduction

Projectile breakup is essential in reactions of weakly-bound nuclei and appears as a strong coupling effect between elastic and breakup channels. The continuum-discretized coupled-channels method (CDCC) was proposed for treating various kinds of channels including breakup (continuum) channels [1–3]. The coupling effect was first confirmed in deuteron scattering and later verified in halo nuclei near the drip-line in which a two-body projectile + target (T) three-body problem was assumed. Nowadays, CDCC is widely applied to describe three-body dynamics.

Our interest is now going to four-body dynamics in scattering of three-body projectiles. CDCC for three- and four-body scattering are now called three- and four-body CDCC, respectively. It is interesting to consider the difference of four-body scattering between ${}^6\text{He}$ and ${}^6\text{Li}$ as typical examples. Since ${}^6\text{He}$ is a Borromean nucleus in which no binary subsystem is bound, only a four-body channel (${}^6\text{He} + T \rightarrow n + n + \alpha + T$) exists as a breakup channel. This property makes four-body dynamics relatively simpler and this is the reason why four-body CDCC was first applied to ${}^6\text{He}$ scattering [4, 5]. On the other hand, ${}^6\text{Li}$ has a bound state in the $n + p$ subsystem. Therefore, not only a four-body channel (${}^6\text{Li} + T \rightarrow n + p + \alpha + T$) but also a three-body channel (${}^6\text{Li} + T \rightarrow d + \alpha + T$) exists in its breakup channel. This situation makes it more difficult to understand four-body dynamics of ${}^6\text{Li}$ scattering.

^ae-mail: s-watanabe@phys.kyushu-u.ac.jp

${}^6\text{Li} + {}^{209}\text{Bi}$ scattering near the Coulomb barrier energy ($E_b^{\text{Coul}} \approx 30$ MeV) was first analyzed with three-body CDCC based on the $d + \alpha + {}^{209}\text{Bi}$ three-body model [6]. However, the calculation could not reproduce the measured elastic cross section without a normalization factor 0.8 to d - ${}^{209}\text{Bi}$ and α - ${}^{209}\text{Bi}$ optical potentials. This problem was solved by four-body CDCC based on the $n + p + \alpha + {}^{209}\text{Bi}$ four-body model [7]. The calculation well describes the experimental data with no adjustable parameter. As an interesting result, it was reported that d breakup in ${}^6\text{Li}$ is strongly suppressed during the elastic scattering. In this work, we focus on four-body dynamics of ${}^6\text{Li}$ elastic scattering from the point of view of four- and three-body channel coupling effects.

2 Theoretical framework and Model Hamiltonian

We recapitulate four-body CDCC based on the $n + p + \alpha + \text{T}$ four-body model; see Ref. [3, 7] for the detail. The scattering state Ψ with the total energy E is governed by the four-body Schrödinger equation with the model Hamiltonian H_4 :

$$(H_4 - E)\Psi = 0, \quad H_4 = K_R + U_n + U_p + U_\alpha + \frac{e^2 Z_{\text{Li}} Z_{\text{T}}}{R} + h_{np\alpha}, \quad (1)$$

where K_R stands for the kinetic energy operator with respect to the relative coordinate \mathbf{R} between ${}^6\text{Li}$ and T, and U_x ($x = n, p, \alpha$) represents the optical potential between x and T. Since Coulomb-breakup effects are negligibly small for the present elastic scattering [6, 7], the Coulomb part of U_p and U_α is then approximated into $e^2 Z_{\text{Li}} Z_{\text{T}} / R$, where Z_A is the atomic number of nucleus A . $h_{np\alpha}$ denotes the internal Hamiltonian of ${}^6\text{Li}$ in the three-cluster model. In CDCC, Eq. (1) is solved in the model space P spanned by the ground and discretized continuum states of ${}^6\text{Li}$:

$$P = \sum_{\gamma=0}^N |\Phi_\gamma\rangle \langle \Phi_\gamma|, \quad (2)$$

where Φ_γ represents the γ -th eigenstate with eigenenergy ε_γ ; note that the $\gamma = 0$ and $\gamma = 1-N$ correspond to the ground and excited states in P , respectively. The Φ_γ are obtained by diagonalizing $h_{np\alpha}$ with the Gaussian basis functions [8].

In order to disentangle breakup dynamics, we divide the CDCC model space P in the following way. P can be decomposed into the ground-state part P_0 and the breakup-state part P^* as $P = P_0 + P^*$ for

$$P_0 = |\Phi_0\rangle \langle \Phi_0|, \quad P^* = \sum_{\gamma=1}^N |\Phi_\gamma\rangle \langle \Phi_\gamma|. \quad (3)$$

For later discussion, P^* is further divided into a subspace $P_{np\alpha}$ dominated by $np\alpha$ configurations and a subspace $P_{d\alpha}$ by $d\alpha$ configurations. The subspaces are defined as follows. The probability of $d\alpha$ configurations in the breakup state Φ_γ is obtained by the overlap between Φ_γ and the d ground state $\phi^{(d)}$: $\Gamma_\gamma^{(d\alpha)} = |\langle \phi^{(d)} | \Phi_\gamma \rangle|^2$. We then define a breakup state with $\Gamma_\gamma^{(d\alpha)} > 0.5$ ($\Gamma_\gamma^{(d\alpha)} \leq 0.5$) as a $d\alpha$ -dominant ($np\alpha$ -dominant) state. The subspace $P_{d\alpha}$ ($P_{np\alpha}$) is a model space spanned by $d\alpha$ -dominant ($np\alpha$ -dominant) breakup states. Consequently, the model space P of CDCC calculations is expressed as

$$P = P_0 + P_{d\alpha} + P_{np\alpha}. \quad (4)$$

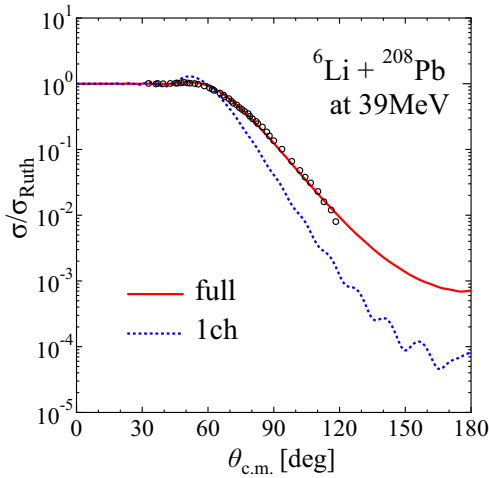


Figure 1. (Color online) Elastic cross sections (normalized by the Rutherford cross section) for ${}^6\text{Li} + {}^{208}\text{Pb}$ scattering at 39 MeV. The solid line represents the result of four-body CDCC calculation with full channel coupling, whereas the dotted line shows the result of 1ch calculation with no channel coupling. The experimental data is taken from Ref. [11].

3 Results

We only show the results of ${}^6\text{Li} + {}^{208}\text{Pb}$ elastic scattering at 39 MeV; see Ref. [7] for the analysis of ${}^6\text{Li} + {}^{209}\text{Bi}$ scattering and the detail of model setting. As for U_n , we take the potential of Koning and Delaroche [9] determined from the measured elastic cross section of $n + {}^{209}\text{Bi}$. For simplicity, the spin-orbit interaction is neglected and U_p is assumed to have the same geometry as U_n . The potential U_α is taken from Ref. [10] determined from measured differential cross sections of $\alpha + {}^{209}\text{Bi}$ scattering at 19–22 MeV.

The angular distribution of elastic cross sections for ${}^6\text{Li} + {}^{208}\text{Pb}$ scattering at 39 MeV are plotted in Fig 1. The one-channel (1ch) calculation with no breakup (dotted line) underestimates the experimental data, whereas the four-body CDCC calculation (solid line) reproduces the experimental data. The enhancement from the dotted to solid lines is induced by channel coupling effects, indicating ${}^6\text{Li}$ breakup effects are quite important. Thus, ${}^6\text{Li}$ scattering on heavy targets are well described by four-body CDCC with no adjustable parameter.

Next, we consider four- and three-body channel coupling effects on the present ${}^6\text{Li}$ scattering. For this purpose, the subspaces $P_{d\alpha}$ and $P_{np\alpha}$ are switched off from the full calculation, respectively. Figure 2 shows the angular distribution for ${}^6\text{Li} + {}^{208}\text{Pb}$ scattering at 39 MeV, and the solid and dotted lines are the same as in Fig. 1. When the model space is limited to $P_0 + P_{np\alpha}$, the dot-dashed line is obtained [see Fig. 2(a)] and close to the result of 1ch calculation (dotted line). On the other hand, when the model space is limited to $P_0 + P_{d\alpha}$, we have the dashed line [see Fig. 2(b)] that well simulates the full calculation (solid line). Note that the number of $d\alpha$ -dominant states in P is as few as about one-eighth of that of $np\alpha$ -dominant states. The result indicates that the coupling between P_0 and $P_{d\alpha}$ is dominant. In other words, ${}^6\text{Li}$ breakup is mainly induced by the $d + \alpha$ breakup, and the d -breakup is suppressed in ${}^6\text{Li}$ scattering.

4 Summary

We have analyzed the four-body dynamics of ${}^6\text{Li}$ elastic scattering. The elastic scattering of ${}^6\text{Li} + {}^{208}\text{Pb}$ at 39 MeV is well described by four-body CDCC based on the $n + p + \alpha + {}^{208}\text{Pb}$ model. The breakup channels are approximately divided into four- and three-body channels and the coupling effects are estimated. ${}^6\text{Li}$ breakup is mainly caused by a strong transition between the elastic (P_0)

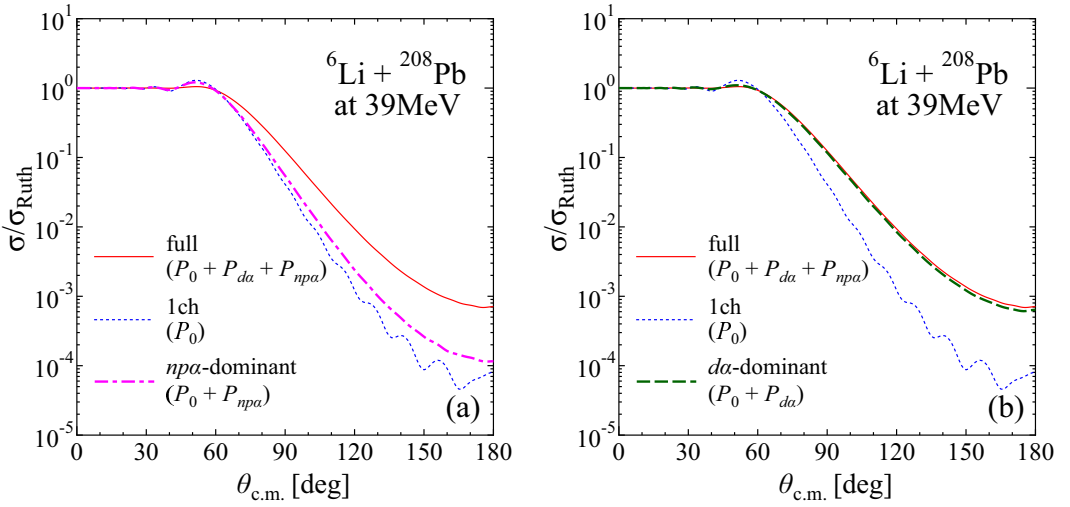


Figure 2. (Color online) Elastic cross sections (normalized by the Rutherford cross section) for ${}^6\text{Li} + {}^{208}\text{Pb}$ scattering at 39 MeV. The solid (dotted) line represents the result of full (1ch) calculation. The dot-dashed line in the panel (a) shows the calculation in which the model space is limited to $P_0 + P_{np\alpha}$, whereas the dashed line in the panel (b) denotes the one with $P_0 + P_{d\alpha}$.

and three-body channel ($P_{d\alpha}$), suggesting d -breakups effect are suppressed in ${}^6\text{Li}$ scattering. We will investigate what causes the suppression, and the energy and target dependence in the forthcoming paper.

Acknowledgements

This work was supported in part by Grant-in-Aid for Scientific Research (KAKENHI) from Japan Society for the Promotion of Science 25-4319.

References

- [1] M. Kamimura *et al.*, Prog. Theor. Phys. Suppl. **89**, 1 (1986)
- [2] N. Austern *et al.*, Phys. Rep. **154**, 125 (1987)
- [3] M. Yahiro *et al.*, Prog. Theor. Exp. Phys. **2012**, 01A206 (2012)
- [4] T. Matsumoto *et al.*, Phys. Rev. C **70**, 061601(R) (2004)
- [5] T. Matsumoto *et al.*, Phys. Rev. C **73**, 051602(R) (2006)
- [6] N. Keeley *et al.*, Phys. Rev. C **68**, 054601 (2003)
- [7] S. Watanabe *et al.*, Phys. Rev. C **86**, 031601(R) (2012)
- [8] E. Hiyama, Y. Kino, and M. Kamimura, Prog. Part. Nucl. Phys. **51**, 223 (2003)
- [9] A. J. Koning and J. P. Delaroche, Nucl. Phys. A **713**, 231 (2003)
- [10] A. R. Barnett and J. S. Lilley, Phys. Rev. C **9**, 2010 (1974)
- [11] S. Santra *et al.*, Phys. Rev. C **83**, 034616 (2011)